

Optimizing The Organic/Inorganic Barrier Structure For Flexible Plastic Substrate Encapsulation

Yi-Chiuan Lin¹, Quoc-Khoa Le¹, Li-Wei Lai², Ren-Mao Liao¹, Ming-Shin Jeng¹, and Day-Shan Liu^{1,*}

¹ Institute of Electro-Optical and Materials Science, National Formosa University, Huwei, Yunlin, Taiwan, ROC.

² ITRI South, Industrial Technology Research Institute, Liujia Shiang, Tainan, Taiwan, ROC.

Received 18 April 2012; received in revised form 20 May 2012; accepted 27 June 2012

Abstract

A multilayered barrier structure stacked with organosilicon and silicon oxide (SiO_x) films consecutively prepared using plasma-enhanced chemical vapor deposition (PECVD) was developed to encapsulate flexible plastic substrate. The evolution on the residual internal stress, structural quality of the organosilicon/SiO_x multilayered structure as well as its adhesion to the substrate were found to correlate closely with the thickness of the inset organosilicon layer. Due to the significant discrepancy in the thermal expansion coefficient between the substrate and SiO_x film, the thickness of the organosilicon layer deposited onto the substrate and SiO_x film thus was crucial to optimize the barrier property of the organosilicon/SiO_x structure. The organosilicon/SiO_x barrier structure possessed a lowest residual compressive stress and quality adhesion to the substrate was achieved from engineering the organosilicon layer thickness in the multilayered structure. The relaxation of the residual internal stress in the barrier structure led to a dense SiO_x film as a consequence of the enhancement in the Si-O-Si networks and thereby resulted in the reduction of the water vapor permeation. Accordingly, a water vapor transmission rate (WVTR) below 1×10^{-2} g/m²/day being potential for the application on the flexible optoelectronic device packaging was achievable from the 3-pairs organosilicon/SiO_x multilayered structure deposited onto the polyethylene terephthalate (PET) substrate.

Keywords: Multilayered barrier structure, organosilicon/SiO_x, plasma-enhanced chemical vapor deposition, flexible plastic substrate, residual internal stress, adhesion, water vapor transmission rate

1. Introduction

Recently, one of the most exciting areas in the flat panel display industry is the emergence of flexible displays. To enable a flexible flat panel display, flexible plastic substrates must be applied to replace conventional glass substrates. However, the limitations of plastic materials in optoelectronic device applications are their permeability of oxygen and moisture [1]. High performance gas barrier coating is therefore indispensable on the surface of plastic substrates. The silicon-based inorganic thin films deposited by plasma-enhanced chemical vapor deposition (PECVD) have been widely used as gas barrier films [2-6]. Although the inorganic materials such as silicon oxide (SiO_x) or silicon nitride (SiN_x) have been shown to have good barrier performance, a technological challenge is the large internal stress resided in the barrier structure while deposited onto the flexible plastic substrate, which can adversely affect the coating/substrate interface and therefore result in the crack or ablation

* Corresponding author. E-mail address: dsliu@sunws.nfu.edu.tw

Tel.: +886-5-6315665; Fax: +886-5-6329257

of a thin film [7]. Accordingly, several researches attempt to control the residual internal stress in the thin film materials at an elevated temperature [8-11]. For instant, Morin et al. reported that high deposition temperature (ca. 1000 °C) was capable to effectively relax the intrinsic stress in SiN_x thin films [9]. Cianci et al. used lower temperature (ca. 500°C) post-deposition thermal treatment to reduce the compressive stress of PECVD-deposited SiN_x films [10]. However, the heat treatment methodology to adjust the residual internal stress of a coating structure is not suitable for low heat-resistant plastic substrates.

Currently, an organic/inorganic multilayered structure consisting of hard inorganic films and soft organic films is comprehensively developed to realize an effective barrier structure prepared onto the plastic substrate [12-16]. In such a multilayered structure, the inorganic layer acts as diffusion barriers to water/oxygen permeation and the organic layer decouples defects in the inorganic layer. Therefore, ultra-high barrier properties is expected to be achieved by using a stacked organic/inorganic structure. However, since the residual internal stress is general a combination of each coating layer [17-18], the increase in the organic/inorganic multilayered structure prepared at a low temperature therefore will lead to the accumulation of the residual internal stress, resulting in the failure of the multilayered structure coated on the flexible plastic substrate. Accordingly, a method to engineer pairs of the low-temperature deposited organic/inorganic multilayered structure is demanded to optimize the coating reliability and barrier property.

In terms of the barrier property, although some researches had demonstrated that the large internal stress resided in the coating structure while deposited onto the flexible plastic substrate was the main factor to limit the resulting water vapor transmission rate (WVTR) [19-21], a systematic study on the relationship between the residual internal stress, adhesion behavior, and barrier property to water vapor permeation of an organic/inorganic multilayered barrier structure coated onto the flexible plastic substrate was rarely discussed.

In this study, with the aim to engineer the internal stress resided in the organic/inorganic barrier structure deposited onto the flexible plastic substrate and investigate its adhesion and barrier property, an organosilicon/SiO_x multilayered barrier structure consecutively deposited onto the PET substrate using the same silicon-based monomer in one PECVD chamber was prepared by altering the organosilicon layer thickness. The residual internal stress, adhesion, and WVTR as a function of the organosilicon layer thickness in the multilayered barrier structure were measured and investigated. The evolution of these coating properties resulted in the change in the chemical bond nature and surface morphology were also conducted and discussed.

2. Experimental

Liquid tetramethylsilane (TMS; Si(CH₃)₄) monomer with a high vapor pressure at room temperature ($\sim 7.1 \times 10^4$ Pa), which has the advantages of deposition security, nontoxicity, and the cost benefit on the fabrication equipments over other precursors, such as SiH₄, TEOS, and HMDSO, was used as the main silicon precursor to consecutively deposit the organosilicon/SiO_x multilayered gas barrier structure onto the (180±10%) μm-thick polyethylene terephthalate (PET) and silicon substrates using a parallel plate capacitatively coupled radio-frequency (13.56 MHz) discharge PECVD system (hereafter referred to as TMS-PECVD). The organosilicon layer and inorganic SiO_x film were respectively synthesized from TMS monomer and TMS-oxygen gas mixture. To engineer the residual internal stress in the organosilicon/SiO_x multilayered structures, the thickness of the inset organosilicon layer was varied and the thickness of the SiO_x film was controlled at 300 nm

which performed a lowest WVTR of 0.34 g/m²/day while directly deposited onto the PET substrate. The pressure, rf power, and substrate temperature to prepare these barrier structures were controlled at 13 Pa, 70 W, and 120°C, respectively. The flow rate of the TMS monomer to prepare organosilicon layer was 60 sccm and the gas flow rate of the TMS-O₂ gas mixture (TMS/O₂) to synthesize SiO_x film was 60/120 sccm.

Film thickness was measured by using a surface profile system (Dektak 6M, Veeco). The chemical bonding states of these barrier structures were examined using a Fourier transform infrared (FTIR) spectrometry (FT/IR-4100, JASCO). The surface morphologies of the barrier structures were observed by a field emission scanning electron microscopy (FE-SEM; JSM-7500F, JEOL). The adhesion behavior between the barrier structure and the PET substrate was evaluated by the ASTM (American Society for Testing and Materials) D3359 standard tape-peeling test [22]. The internal stress, σ_f , resided in the barrier structure with a thickness, d_f , was measured by the beam bending method using a thin film stress measurement instrument (FLX-2320, Tencor), and derived from the Stoney formula expressed as [23]:

$$\sigma_f = \frac{E_s d_s^2}{6(1-\nu_s) d_f} \left(\frac{1}{R_f} - \frac{1}{R_0} \right) \quad (1)$$

where E_s , ν_s , and d_s are Young's modulus, Poisson ratio, and thickness of the silicon substrate, respectively. R_0 and R_f are the radii of the sample curvature before and after the barrier structure deposition. The water vapor permeation of the bare and coated PET substrates was measured using a WVTR measurement system (PERMATRAN-W 3/61, MOCON Inc.) at a temperature of 40°C with 95% relative humidity (RH).

3. Results and discussions

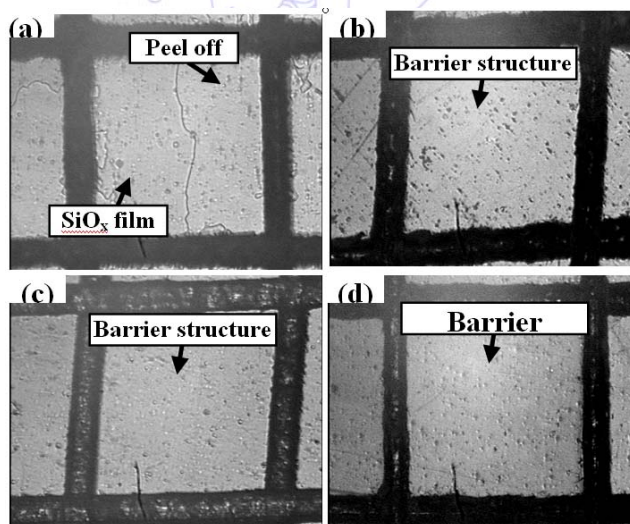


Fig. 1 Tape-peeling tests observed by an optical microscope for the (a) SiO_x gas barrier layer and multilayered structures with an organosilicon layer of (b) 15, (c) 30, and (d) 60 nm, respectively, deposited onto the PET substrate.

Fig. 1(a)-(d) show the tape-peeling tests observed by an optical microscope for the gas barrier structures with and without an organosilicon layer of 15, 30, and 60 nm, respectively. The 300-nm SiO_x film directly deposited onto the PET substrate, as shown in Fig. 1(a), was almost completely peeled off due to the significant difference in the material properties and the poor contact between the inorganic barrier film and plastic substrate, as documented elsewhere [24]. By inseting the

organosilicon layer, none of the cross-cut area for the organosilicon/SiO_x multilayered structure was peeled off the PET substrate (as shown in Fig. 1(b), (c), and (d)). According to the ASTM D3359 standard tape-peeling test, the adhesion levels of these barrier structures were all evaluated as rank 5B (no peel-off; none of the squares were detached).

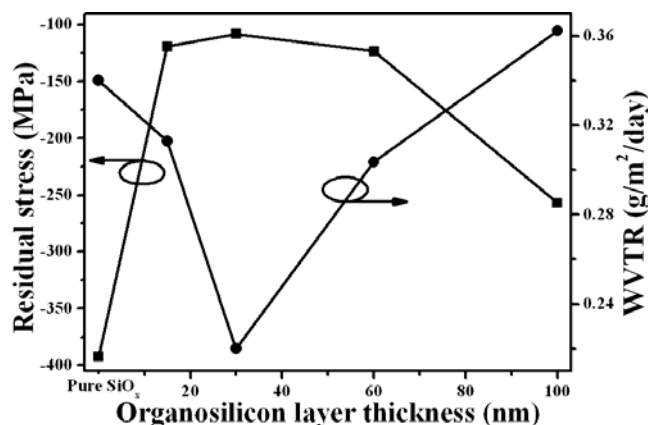


Fig. 2 Residual internal stress and WVTR of the multilayered barrier structures as a function of the organosilicon layer thickness.

The residual internal stress and WVTR of these barrier structures coated onto the substrate as a function of the organosilicon layer thickness are shown in Fig. 2. It was clearly seen that the SiO_x film directly deposited on the silicon substrate, which was almost completely peeled off the PET substrate after tape-peeling test, had a large residual compressive stress of -392 MPa. When the organosilicon layer inset between the SiO_x film and the substrate, the residual compressive stress in the gas barrier structure was effectively reduced, revealing that the organosilicon layer facilitated to buffer the stress resided in the SiO_x film. In addition, although the organosilicon/SiO_x structures were all well adherent to the PET substrate as observed from their tape-peeling tests, the internal stress residing in the barrier structures showed slight variations. A lowest compressive stress (-108 MPa) was achieved from the gas barrier structure with an organosilicon layer thickness of 30 nm, and it was gradually increased by increasing the organosilicon layer thickness in the multilayered structure. The gas barrier structure to the water vapor permeation was found to be closely correlated with the residual internal stress evolution. The lower the compressive stress resided in the gas barrier structure, the better the WVTR is obtained, indicating that the SiO_x barrier property could be further optimized by controlling the residual stress in the multilayered structure with an adequate thickness of the organosilicon layer. The main chemical bonds in these barrier structures deposited onto the silicon substrates were measured to further investigate the structural evolutions of the SiO_x film affected by inseting the organosilicon layer.

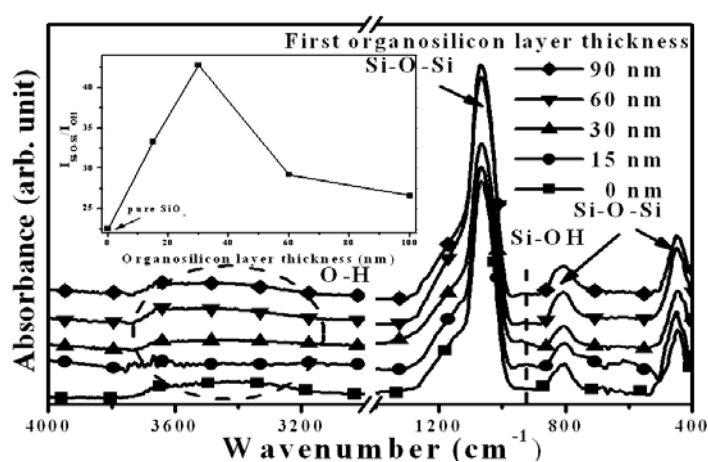


Fig. 3 FTIR spectra of the multilayered barrier structures as a function of the organosilicon layer thickness (the relative intensity ratio ($I_{Si-O-Si}/I_{OH}$) is shown in inset figure).

Fig. 3 shows the FTIR spectra of the single SiO_x film and the organosilicon/ SiO_x multilayered structures with an organosilicon layer thickness of 15, 30, 60, and 90 nm, respectively. For the FTIR spectrum of the 300 nm-thick SiO_x film directly deposited onto the substrate, the absorbance peaks located at approximately 1058, 795, and 447 cm^{-1} emerged from the Si-O-Si stretching, bending, and rocking modes, where the broad peak at around 3200–3700 cm^{-1} and the weak peak at 925 cm^{-1} were identified as the hydroxyl (-OH) and silanol (Si-OH) chemical bonds, respectively [25-26]. The appearance of the OH groups was related to both the porous structure in the SiO_x films and surface-adsorbed H_2O , and also was demonstrated as the hydrophilic group [27-28]. Clearly, the bond types and peak positions of the multilayered barrier structure showed no apparent difference from the single SiO_x film except for the relative intensity ratio of the Si-O-Si stretching mode to hydroxyl bond ($I_{\text{Si-O-Si}}/I_{\text{OH}}$), indicating that the inseting thin organosilicon layer only led to the change in the porous distribution of the consecutively deposited SiO_x film. The FTIR spectrum of the SiO_x film deposited onto a 30 nm-thick organosilicon layer exhibited the most intense Si-O-Si signal than other barrier structures, as shown in the inset figure, implying the achievement of a good SiO_x structural quality and film densification, which also resulted in the lowest WVTR value and residual internal stress, as shown in Fig. 2. By contrast, the decreased relative intensity ($I_{\text{Si-O-Si}}/I_{\text{OH}}$) emerged from the multilayered gas barrier structure with an organosilicon layer thickness reaching 60 nm demonstrated the inferior SiO_x film quality, consistent with the degradation of the barrier performance to vapor permeation.

The organosilicon layer plasma-polymerized from TMS monomer which was abundant in the C-H chemical bonds was suggested to be responsible for the increase in the SiO_x film quality. Since the organosilicon layer surface featured as the hydrophobic C-H chemical bonds corresponded to a low surface energy ($\sim 12 \text{ J/m}^2$) [20], the inert surface was thus beneficial to lower the adsorption of the ambient contaminants. Especially for the water vapor resided in the vacuum chamber and/or synthesized from plasma deposition that discharged OH free radicals and caused the deposited SiO_x film with terminated Si-OH defects. Accordingly, the surface energy of the organosilicon layer lower than that of the bare PET substrate surface ($\sim 26 \text{ J/m}^2$) was more effective in attaining a dense and finer structure in the subsequently deposited SiO_x film due to the increase in the density of the nucleation sites in the region of initial growth, consistent with the earlier reports that discussed a thin film deposited on the surface modification layer [29-31].

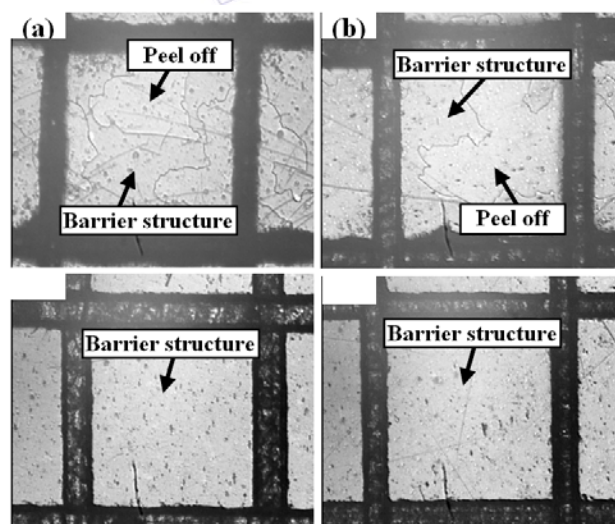


Fig. 4 Micrographs of the tape-peeling test results for the 2-pairs multilayered barrier structures with the second organosilicon layer thickness of (a) 15, (b) 30, (c) 60, and 90 nm respectively, deposited onto the PET substrate.

After we optimized the residual internal stress of the SiO_x film deposited onto the substrate by inseting a 30 nm-thick organosilicon layer, which also have the best barrier property for water vapor permeation, an attempt to stack the

organosilicon/SiO_x multilayered structure encapsulate the PET substrate to further reduce the resulting WVTR was carried out. Fig. 4(b) shows the optical microscopy of the tape-peeling test results for the barrier structure stacked from a 2-pairs organosilicon (30 nm)/SiO_x (300 nm) multilayered barrier structure coated on the PET substrate. Evidently, such 2-pairs multilayered barrier structure exhibited poor adhesion to the PET substrate, implying that the thickness of the second organosilicon layer should be further designed to stack a quality pairs of the multilayered barrier structures.

Fig. 4(a)-(d) illustrate the micrographs of the tape-peeling test results for the 2-pairs multilayered barrier structures with the second organosilicon layer thickness of 15, 30, 60, and 90 nm, respectively. It was found that the 2-pairs barrier structure with the second organosilicon layer thickness of 15 and 30 nm exhibited poor adhesion to the PET substrate (ranked as 2-3B according to ASTM D3359), whereas the barrier structures stacked with the second organosilicon layer thickness of 60 and 100 nm, respectively, adhered well to the PET substrate (ranked as 5B).

Similar to the well correlation between the adhesion and residual internal stress of the 1-pair organosilicon/SiO_x barrier structures deposited onto the substrates, the adhesion of these 2-pairs barrier structures constructed from different thickness of the second organosilicon layer were also linked to the evolution of their residual internal stress. In theory, for a multilayered structure of n films having thickness $t_1, t_2, t_3, \dots, t_n$ each of which develops a stress $S_1, S_2, S_3, \dots, S_n$, the average residual internal stress S can be evaluated as the following equation [32]:

$$S = \frac{S_1 t_1 + S_2 t_2 + S_3 t_3 + \dots + S_n t_n}{t_1 + t_2 + t_3 + \dots + t_n} \quad (2)$$

As referred from the residual internal stress of the single SiO_x (-392 MP) film and organosilicon (30 nm)/SiO_x (300 nm) multilayered structure (-108 MPa) deposited onto the substrates, the residual internal stress of the 30 nm-thick organosilicon layer deposited onto the substrate was calculated as a tensile stress of 2732 MPa. According to Eq. (2), a lowest residual internal stress was also expected to be obtained from the 2-pairs organosilicon/SiO_x multilayered structure with each organosilicon layer thickness of 30 nm. However, due to the surface and material properties of the film such as the surface roughness, surface energy, and thermal expansion coefficient are quite different from that of the substrate, giving rise to different nucleation condition for the subsequently deposited film, it was hardly possible to acquire the average stress of the multilayered structure from the stress found in the initial multilayered structure by using Eq. (2) [32-33].

Accordingly, the optimal thickness of the organosilicon layer in the 1-pair organosilicon/SiO_x multilayered structure that performed a lowest residual internal stress might not be the critical thickness of the second organosilicon layer in the 2-pairs barrier structures since the surface and material properties for the second-organosilicon layer deposition were significantly different from that of the first layer deposited onto the substrate.

Fig. 5 shows the residual internal stress of the 2-pairs organosilicon/SiO_x multilayered structures as a function of the second organosilicon layer thickness. The residual internal stress of these 2-pairs multilayered structures was decreased with increasing the thickness of the second organosilicon layer, and a lowest compressive stress of 217 MPa was achieved from the structure with a second organosilicon layer of 60 nm which also exhibited the quality adhesion (ranked 5B) to the substrate.

For the second organosilicon layer thickness reached 100 nm, although the adhesion between the barrier structure and the substrate was still ranked 5B, the compressive stress resided in the 2-pairs organosilicon/SiO_x structure was again increased to 239 MPa. The WVTR of these 2-pairs barrier structures also was found to be well correlated with the evolution of the residual internal stress. The small the residual internal compressive stress, the better the resulting WVTR for the 2-pairs barrier structure coated onto the PET substrate is. A lowest WVTR of 0.08 g/m²/day was achievable from the 2-pairs

organosilicon/SiO_x barrier structure with the second organosilicon layer thickness of 60 nm, whereas a WVTR of about 0.19 g/m²/day was measured from the 2-pairs barrier structure having the same organosilicon layer thickness of 30 nm. The associated FTIR spectra of these 2-pairs barrier structures as a function of the second organosilicon layer thickness are illustrated in Fig. 6. All these barrier structures were constructed from the Si-O-Si networks and featured of the porous-related OH groups. The Si-O-Si stretching peak position emerged from the 2-pairs barrier structures shifted towards a higher wavenumber of 1074 cm⁻¹ as compared to that of the 1-pair barrier structures (~ 1064 cm⁻¹) shown in Fig. 3.

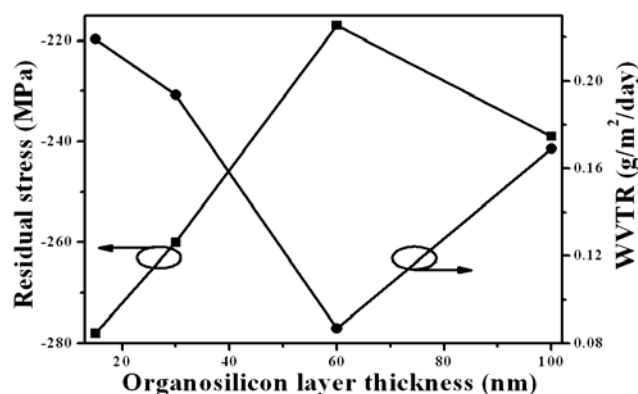


Fig. 5 Residual internal stress and WVTR of the 2-pairs multilayered barrier structures as a function of the second organosilicon layer thickness.

Such peak shift had been demonstrated as the change in the Si-O-Si bond angle accompanied by a more SiO₂-like character of the structure [34-35]. In addition, a largest relative intensity ratio ($I_{Si-O-Si}/I_{OH}$) also was obtained from the 2-pairs barrier structure with the second organosilicon layer of 60 nm, as shown in the inset figure, indicating the densification of the Si-O-Si network and also resulting in the improvement on the barrier property to water vapor permeation. In terms of the internal stress resided in the coating structure, the residual internal stress of a coating system is a combination of the intrinsic stress and thermal stress. The intrinsic stress is related to the internal structure and element composition, whereas the thermal stress arises from the thermal expansion mismatch between the coating and the substrate.

Since reports had pointed out that the compressive stress relaxation in the coating was due to the hydrogenated bond dissociation [33, 36], the evolution of the organosilicon/SiO_x multilayered structure on the residual internal stress shown in Fig. 2 and Fig. 5, thus were deeply correlated with the relative intensity ratio of the Si-O-Si stretching mode to hydroxyl bond and also led to the improvement in the barrier property due to the increase in the crosslinked Si-O-Si network. In addition, due to the significant difference in the thermal stress induced from the organosilicon layer deposited onto the silicon substrate and the SiO_x film which has the thermal expansion coefficient of the $0.4 \times 10^{-6} \text{ K}^{-1}$ and $2.3 \times 10^{-6} \text{ K}^{-1}$, respectively, the second organosilicon layer thickness required to buffer the compressive stress of the SiO_x barrier film thus was different from that of the first organosilicon layer thickness (ie. a thickness of 60 nm that was doubly thicker than that of the first organosilicon layer of 30 nm). Accordingly, the thickness of the 2nd, 3rd, 4th, and nth organosilicon layer while deposited onto the SiO_x layer to buffer the structure residual compressive stress was designed as 60 nm.

As the thickness of the organosilicon layer deposited onto the substrate and silicon film to release the residual internal stress in the organosilicon/SiO_x multilayered structure which corresponded to the excellent adhesion and lowest WVTR had been optimized, the preparation for pairs of the organosilicon/SiO_x multilayered barrier structures suitable for flexible optoelectronic packaging was carried out.

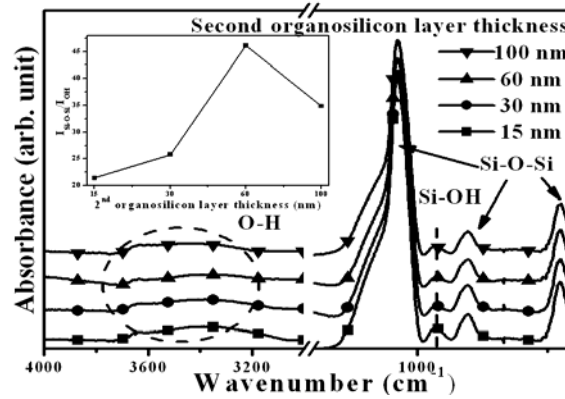


Fig. 6 Residual internal stress and WVTR of the 2-pairs multilayered barrier structures as a function of the second organosilicon layer thickness.

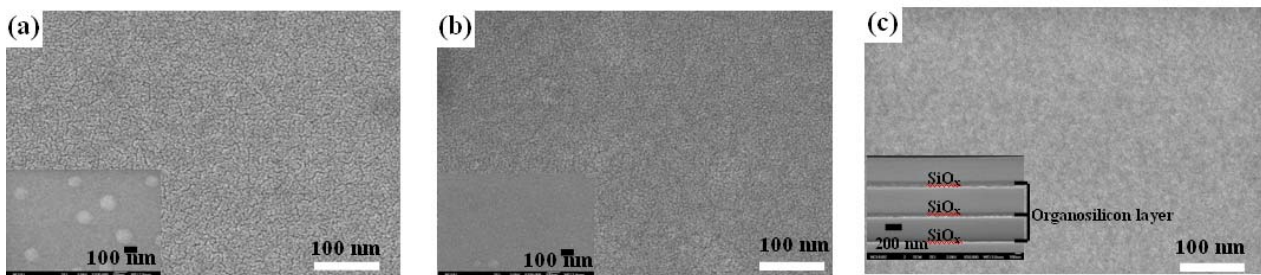


Fig. 7 Surface morphologies of the (a) single SiO_x , (b) 1-pair, and (c) 3-pairs organosilicon/ SiO_x multilayered barrier structures (the inset figures in Fig. 7(a) and (b) are low magnification photographs and the inset figure in Fig. 7(c) is a cross-sectional micrograph of the 3-pairs barrier structure).

Figure 7 (c) shows the surface morphology of the 3-pairs barrier organosilicon/ SiO_x multilayered barrier structure observed by FE-SEM. The thickness of the 1st, 2nd, and 3rd organosilicon layer (30, 60, and 60 nm, respectively) also can be seen in the cross-sectional micrograph inset in Fig. 7(c). In addition, the surface morphologies of the single SiO_x film and 1-pairs organosilicon/ SiO_x structure with the organosilicon layer of 30 nm are given in Fig. 7(a) and (b), respectively. As can be seen in Fig. 7(a), the SiO_x barrier film directly deposited onto the substrate performs a surface morphology with well-defined boundaries. Such boundaries were indicative of the macro- or micro-sized defects in the single SiO_x barrier that were demonstrated as additive penetrated paths of gases into the film, thereby limiting the barrier behavior of the single SiO_x film [37-39]. The inset figure observed at low magnification also shows the surface defects of white protrusions. By contrast, the surface morphology of the SiO_x films deposited onto a 30 nm-thick organosilicon layer, as shown in Fig. 7(b), showed a dense feature with fine size distribution.

The improvement in the Si-O-Si networks and the release of residual internal stress led to the decrease of the protrusions as observed in the inset figure. In agreement with the report which demonstrated that the defects in the inorganic layer were prone to be decoupled by the presented organic layer [40], the surface morphology of the 3-pairs barrier structure thus was free from the white protrusions. In addition, the organosilicon layer and SiO_x film shown in the inset figure were well defined without apparent pinholes and cracks, thereby facilitating the enhancement in the barrier performance. The barrier parameters relate to the barrier improvement factor (BIF) and effective permeability of the single SiO_x , 1-pair, 2-pairs, and 3-pairs organosilicon/ SiO_x multilayered barrier structures deposited on the PET substrate as well as the PET substrate is summarized in Table 1 (the thickness of the 1st, 2nd, and 3rd organosilicon layer thickness was 30, 60, and 60 nm, respectively). The effective permeability, P_c , for the coating structure with the effect of the PET substrate eliminated was derived from the following equation using Ideal Laminate Theory (ILT) [41]:

$$\frac{1}{\Pi_T} = \frac{d_T}{P_T} = \frac{d_s}{P_s} + \frac{d_c}{P_c} \quad (3)$$

where Π is the transmission rate, P is permeability, d is thickness, and s, c and T are the substrate, coating and the composite structure (s + c), respectively. In addition, BIF is defined as the ratio of WVTR of the substrate (Π_s) to the coated substrate (Π_T). In terms of the barrier performance, the 1-pair barrier structure with a 30 nm-thick organosilicon film showed a significant reduction in the effective permeability ($\sim 0.077 \mu\text{m-g/m}^2/\text{day}$) as compared to the single 300 nm-thick SiO_x film deposited directly onto the PET substrate ($\sim 0.112 \mu\text{m-g/m}^2/\text{day}$), implying that the barrier property of the SiO_x film itself was further improved by inseting such organosilicon layer. By coating a 2-pairs barrier structure on the PET substrate, the WVTR was further reduced to $0.08 \text{ g/m}^2/\text{day}$, corresponding to the effective permeability and BIF of $0.056 \mu\text{m-g/m}^2/\text{day}$ and 47.5, respectively. When the multilayered barrier structure coated onto the PET substrate reached three pairs, the resulting WVTR was sharply decreased to a value below the MOCON detection limit ($< 1 \times 10^{-2} \text{ g/m}^2/\text{day}$), indicating that the designed pairs organosilicon/ SiO_x barrier structure is a promising candidate for packaging the flexible optoelectronic devices.

4. Conclusions

In this work, we had systematic investigated and discussed on the barrier performance of the stacked organosilicon/ SiO_x multilayered structure consecutively deposited onto the PET substrate by PECVD using TMS monomer and TMS–oxygen gas mixture, respectively, as a function of the organosilicon layer thickness. The large residual compressive stress ($\sim 392 \text{ MPa}$) of the SiO_x film directly deposited onto the substrate was effectively released by inseting organosilicon layer plasma polymerized from TMS monomer, resulting in the apparent improvements on the adhesion and structural densification of the upper SiO_x film. The densest Si-O-Si networks in the SiO_x film deposited onto a 30 nm-thick organosilicon layer assessed from the intensity ratio ($I_{\text{Si-O-Si}}/I_{\text{OH}}$) in the related FTIR spectra, that also possessed a lowest residual compressive stress of 108 MPa, thus resulted in a lower WVTR ($\sim 0.22 \text{ g/m}^2/\text{day}$) than that of the SiO_x film directly coated onto the PET substrate ($\sim 0.34 \text{ g/m}^2/\text{day}$). However, due to the internal residual stress especially for the thermal stress induced from the organosilicon layer deposited onto the substrate and SiO_x was quite different originating from the discrepancy in the thermal expansion coefficient of the substrate and SiO_x film, the 2-pairs organosilicon/ SiO_x structure with the same organosilicon layer thickness of 30 nm would not lead to the lowest residual internal stress and best barrier performance (WVTR $\sim 0.19 \text{ g/m}^2/\text{day}$).

The thickness of the second organosilicon layer required for the multilayered structure possessed the optimal SiO_x structural quality and quality adhesion of 5B was 60 nm, a value doubly thicker than that of the first organosilicon layer, benefiting in improving the degree of WVTR of $0.08 \text{ g/m}^2/\text{day}$ while deposited onto the PET substrate. Accordingly, by stacking the organosilicon/ SiO_x multilayered barrier structure with the organosilicon layer thickness deposited onto the substrate and SiO_x film of 30 and 60 nm, respectively, a WVTR below the commercially-used MOCON instrument detection limit ($\sim 1 \times 10^{-2} \text{ g/m}^2/\text{day}$) was achievable from the 3-pairs organosilicon/ SiO_x multilayered structure. Such stress-controlled organosilicon/ SiO_x multilayered barrier structure by simple optimizing the thickness of the organosilicon layer is a promising barrier structure for the application on the flexible optoelectronic device packaging.

Acknowledgement

This work was supported by the National Science Council and Industrial Technology Research Institute (ITRI South) under no. B200-101WE2. The authors also acknowledge the FE-SEM measurement support from “Common Lab for

Micro/Nano Science and Technology” in National Formosa University.

References

- [1] J. Lange and Y. Wyser, “Recent innovations in barrier technologies for plastic packaging—a review,” *Packaging Technology and Science*, vol. 16, pp. 149-158, Sep. 2003.
- [2] A. Gruniger, A. Bieder, A. Sonnenfeld, Ph. Rudolf von Rohr, U. Muller, and R. Hauert, “Influence of film structure and composition on diffusion barrier performance of SiO_x thin films deposited by PECVD,” *Surface and Coatings Technology*, vol. 200, pp. 4564-4571, Apr. 2006.
- [3] T.T. Pham, J. H. Lee, Y. S. Kim, and G. Y. Yeom, “Properties of Si_xN_y thin film deposited by plasma enhanced chemical vapor deposition at low temperature using SiH₄/NH₃/Ar as diffusion barrier film,” *Surface and Coatings Technology*, vol. 202, pp. 5617-5620, Aug. 2008.
- [4] U. Schulz and N. Kaiser, “Vacuum coating of plastic optics,” *Progress in Surface Science*, vol. 81, pp. 387-401, Aug. 2006.
- [5] P. Morin, E. Martinez, F. Wacquant, and J. L. Regolini in T. E. Buchheit, A. M. Minor, R. Spolenak, and K. Takashima (Eds.), *Thin Films: Stresses and Mechanical Properties XI*, Warrendale, PA, U.S.A., Materials Research Society Symposium Proc., vol. 875, pp. 437, 2005.
- [6] E. Cianci, L. Visigalli, V. Foglietti, G. Caliano, and M. Pappalardo, “Improvements towards a reliable fabrication process for cMUT,” *Microelectronic Engineering*, vol. 67-68, pp. 602-608, Mar. 2003.
- [7] T. N. Chen, D. S. Wu, C. C. Wu, C. C. Chiang, Y. P. Chen, and R. H. Horng, “Improvements of Permeation Barrier Coatings Using Encapsulated Parylene Interlayers for Flexible Electronic Applications,” *Plasma Processes and Polymers*, vol. 4, pp. 180-185, Feb. 2007.
- [8] J. W. Han, H. J. Kang, J. Y. Kim, G. Y. Kim, and D. S. Seo, “Improvement of Permeation of Solvent-Free Multilayer Encapsulation of Thin Films on Poly(ethylene terephthalate),” *Japanese Journal of Applied Physics*, vol. 45, pp. 9203-9204, Dec. 2006.
- [9] G. L. Graff, R. E. Williford, and P. E. Burrows, “Mechanisms of vapor permeation through multilayer barrier films: Lag time versus equilibrium permeation,” *Journal of Applied Physics*, vol. 96, pp. 1840-1849, May 2004.
- [10] N. Sabate, I. Gracia, J. Santander, L. Fonseca, E. Figueras, C. Cane, and J. R. Morante, “Mechanical characterization of thermal flow sensors membranes,” *Sensors and actuators A-Physical*, vol. 125, pp. 260-266, Sep. 2006.
- [11] C.Y. Wu, W.C. Chen, D.S. Liu, 2008, “Surface modification layer deposition on flexible substrates by plasma-enhanced chemical vapour deposition using tetramethylsilane–oxygen gas mixture,” *Journal of Physics D: Applied. Physics*, vol. 41, pp. 225305/1-225305/8, Oct. 2008.
- [12] K. Lau, J. Weber, H. Bartzsch, and P. Frach, “Reactive pulse magnetron sputtered SiO_xN_y coatings on polymers,” *Thin Solid Films*, vol. 517, pp. 3110-3114, Mar. 2009.
- [13] ASTM D3359, *Standard Test Methods for Measuring Adhesion by Tape Test*, ASTM International, West Conshohocken, PA (2008).
- [14] V. Bhatt, S. Chandra, S. Kumar, and P. N. Dixit, “Stress evaluation of RF sputtered silicon dioxide films for MEMS,” *Indian Journal of Pure & Applied Physics*, vol. 45, pp. 382-386, Apr. 2007.
- [15] D. S. Liu, and C. Y. Wu, “Adhesion enhancement of hard coatings deposited on flexible plastic substrates using an interfacial buffer layer,” *Journal of Physics D: Applied. Physics*, vol. 43, pp. 175301/1-175301/10, Apr. 2010.
- [16] K. Teshima, H. Sugimura, Y. Inoue, and O. Takai, “Gas Barrier Performance of Surface-Modified Silica Films with Grafted Organosilane Molecules,” *Langmuir*, vol. 19, pp. 8331-8334, Aug. 2003.
- [17] W. S. Liao and S. C. Lee, “Water- induced room- temperature oxidation of Si–H and –Si–Si– bonds in silicon oxide,” *Journal of Applied Physics*, vol. 80, pp. 1171-1176, Jul. 1996.
- [18] M. Benmalek and H. M. Dunlop, “Inorganic coatings on polymers,” *Surface and Coatings Technology*, vol. 76-77, pp. 821-826, Dec. 1995.
- [19] S. H. Kong, K. Mizuno, T. Okamoto, and S. Nakagawa, “Oxide seed layer with low surface energy to attain fine grains in magnetic layers,” *Journal of Applied Physics*, vol. 93, pp. 6781-6783, May 2003.
- [20] M. A. El Khakani, M. Chaker, A. Jean, S. Boily, H. Pépin, J. C. Kieffer, and S. C. Gujrathi, “Effect of rapid thermal annealing on both the stress and the bonding states of a-SiC:H films,” *Journal of Applied Physics*, vol. 74, pp. 2834-2840, Apr. 1993.

- [21] H. Nakashima, K. Furukawa, Y. C. Liu, D. W. Gao, Y. Kashiwazaki, K. Muraoka, K. Shibata, and T. Tsurushima, "Low-temperature Deposition of High-Quality Silicon Dioxide Films by Sputtering-type Electron Cyclotron Resonance Plasma," *Journal of Vacuum Science and Technology A*, vol. 15, pp. 1951-1954, Jul. 1997.
- [22] D. S. Kim and Y. H. Lee, "Room-temperature deposition of a-SiC:H thin films by ion-assisted plasma-enhanced CVD," *Thin Solid Films*, vol. 283, pp. 109-118, Sep. 1996.
- [23] D. S. Wu, W. C. Lo, C. C. Chiang, H. B. Lin, L. S. Chang, R. H. Horng, C. L. Huang, and Y. J. Gao, "Plasma-deposited silicon oxide barrier films on polyethersulfone substrates: temperature and thickness effects," *Surface and Coatings Technology*, vol. 197, pp. 253-259, Jul. 2005.
- [24] D. G. Howells, B. M. Henry, J. Madocks, and H. E. Assemder, "High quality plasma enhanced chemical vapour deposited silicon oxide gas barrier coatings on polyester films," *Thin Solid Films*, vol. 516, pp. 3081-3088, Mar. 2008.
- [25] G. Dennler, C. Lungenschmied, H. Neugebauer, N. S. Sariciftci, M. Latreche, G. Czeremuszkin, and M. R. Wertheimer, "A new encapsulation solution for flexible organic solar cells," *Thin Solid Films*, vol. 511-512, pp. 349-353, Jul. 2006.

